

Full Length Article

Exploration of operating conditions in the direct aqueous-phase reforming of plastics

C. Ruiz-Garcia, J.A. Baeza^{*}, A.S. Oliveira, S. Roldán, L. Calvo, M.A. Gilarranz*Departamento de Ingeniería Química, C/Francisco Tomás y Valiente 7, Universidad Autónoma de Madrid, 28049 Madrid, Spain*

ARTICLE INFO

Keywords:

Plastic waste

H₂

Aqueous-phase reforming

Pt/C

Operating conditions

ABSTRACT

Plastic materials are employed in countless applications, resulting in a high amount of waste and the need for alternatives to landfill. In the current work, an alternative to reduce and revalorize waste plastic using direct aqueous-phase reforming (APR), a catalytic process to produce hydrogen and/or alkanes from organic molecules, is proposed with a focus on polyethylene terephthalate. The effect of operating conditions including temperature (190–235 °C), pH (3–12), and the type of metal catalyst and support, was studied. Pt catalysts yielded at 220 °C 5 mmol of H₂/g of plastic in 4-hour reaction tests, which increased up to 10 mmol of H₂/g of plastic for an 8-hour reaction time. Additionally, low amounts of short-chain alkanes were detected (<1.4 mmol of alkanes/g of plastic). The production of H₂ was also improved by increasing reaction temperature up to 235 °C, and by using Pt-based bimetallic catalysts and supports with well-developed mesopore area. The results obtained confirm the potential of this strategy as a useful and simple way to transform plastic waste, especially PET, into H₂.

1. Introduction

Plastic materials have taken a crucial role in the development of modern lifestyle due to their versatility, long-life, utility, affordable cost, and intrinsic properties such as inertness and lightweight nature, among others. However, the widespread use of plastic materials, together with their low degradability, has produced a huge environmental challenge [1,2]. The persistence of plastics in the environment promotes the release of plastic particles of all sizes in water, soils, and air [3], provoking negative ecotoxicological effects. They have also been reported to absorb toxic substances and affect all trophic levels in ecosystems, eventually entering the human body through the food chain [2,4]. Beyond these considerations, the impact of plastics on the environment presents an additional consequence, interconnecting plastics and climate change, since the production and degradation of these materials contribute to the generation and release of greenhouse gases [2].

It is calculated that during the period from 1950 to 2017, 7 billion tons of plastic waste ended up in landfills or were dumped. Although a decrease in plastic use was observed in the years before 2020, the demand for single-use items and disposable plastic medical supplies during the COVID-19 pandemic has caused a new impulse to the production of plastics and thus the generation of plastic has increased again [5]. In

2020, in the European Union, 35 % of the plastic waste was recycled, 42 % subjected to energy valorization, and 23 % was disposed of in landfills, indicating the high level of final plastic waste [6]. Globally, only 9 % of plastic is estimated to be recycled, and a large proportion evades waste management systems.

Actions involving the reduction, reuse, and recycling of plastics have made a significant contribution to tackling waste plastic challenges. Some plastics have a chemical structure that makes recycling possible, although some limitations have hampered this option due to high cost and the lack of infrastructure to carry out the process. The substitution of traditional plastics, such as polyethylene terephthalate (PET), polystyrene (PS) or polyethylene (PE), with compostable plastics (i.e. polylactic acid) has contributed to minimizing the environmental impact of plastic usage [7]. However, this option implies a loss of resources and conflicts with the circular economy model, where the principles are to share, reuse, repair, refurbish and recycle, to save raw materials and energy and create new supply chains.

The transition to a circular economy seeks to extend the life cycle of products as much as possible, minimize waste, and contribute to achieving a sustainable model [8]. In this context, new approaches must be developed for plastic materials and products, as their production demands significant quantities of raw materials and generates

^{*} Corresponding author.

E-mail addresses: cristina.ruiz@uam.es (C. Ruiz-Garcia), josealberto.baeza@uam.es (J.A. Baeza), sara.roldang@estudiante.uam.es (S. Roldán), luisa.calvo@uam.es, miguel.gilarranz@uam.es (M.A. Gilarranz).

<https://doi.org/10.1016/j.fuel.2024.132446>

Received 21 January 2024; Received in revised form 3 July 2024; Accepted 5 July 2024

Available online 9 July 2024

0016-2361/© 2024 The Authors. Published by Elsevier Ltd. This is an open access article under the CC BY-NC-ND license (<http://creativecommons.org/licenses/by-nc-nd/4.0/>).

substantial waste that is not returned to the supply chain. Thus, the valorization of plastic waste plays a crucial role in addressing this situation and overcoming bottlenecks in recycling, giving new life to waste through transformation into substances than can be used as commodities for other processes.

In recent years, plastic waste valorization to produce H₂ has gained much attention as an interesting alternative to traditional practices such as incineration, disposal in landfills or direct release into the environment. Thermochemical processes such as catalytic pyrolysis, steam reforming, and their combinations are among the most studied treatment methods [9–12]. These methods typically require moderate (>400 °C) to very high temperatures, sometimes up to 1500 °C, resulting in high energy consumption and environmental impact. Moreover, some plastics are challenging for thermochemical processes. For example, the thermal decomposition of polyethylene terephthalate (PET) leads to phthalic acid that affect pyrolysis oil quality and cause equipment obstructions, consequently limiting PET content to 1–2 % in the plastic waste mixture used as feedstock [13].

Aqueous phase reforming (APR) is a catalytic process for converting water-soluble organic molecules into hydrogen, operating at 170–250 °C, and using supported mono- and bimetallic catalytic systems based on Pt, Pd, Ru, Rh, among other metals, and their combinations [14]. Some authors have successfully explored the reforming of plastics in the aqueous phase. Su et al. [5] developed a coupled process to convert initial PE to more suitable compounds for reforming by hydrothermal oxidation followed by APR, obtaining values of 10 mol H₂/kg_{PE}. Additionally, a process has been described recently that involves the hydrolysis of pure PET, followed by the conversion of the solubilized fraction, principally ethylene glycol, by APR. A H₂ yield of 12.2–23.7 mol per kg_{PET} together with disodium terephthalate as main by-product was reported. The H₂ yield depends on the catalyst employed and the reaction temperature [15]. This interesting approach could present potential limitations when PET is combined with other non-hydrolysable plastics and still requires the assessment of operating conditions. The concept aligns with other works in the literature on using APR for the conversion of solid waste, using a previous solubilization stage since APR strictly occurs in the aqueous phase [16]. However, the reforming of plastics is still in an early stage and is a field to be further explored.

In the current work, we explore the conversion of several plastics to hydrogen, emphasizing the case of PET but also exploring other solid particles of PE and PS through direct APR of their suspensions in water, without prior treatment. These plastics are among the most used commodity plastics, produced in high volumes for applications such as packaging, food containers, etc. Most of them are conceived as single-use products and, therefore, have a significant environmental impact. An exploratory study is conducted to investigate the behavior of the different types of plastic in relation to their structure and to assess the influence of APR operating variables. The feasibility of the one-step APR process for converting plastic to H₂ is examined.

2. Experimental

2.1. Materials

H₂PtCl₆ (8 wt% in H₂O), PdCl₂ (99 %) and RhCl₃ (98 %) were purchased from Sigma-Aldrich. Carbon blacks ENSACO 250G (ENS250) and ENSACO 350G (ENS350) were supplied by TIMCAL Canada Inc. Activated carbon (Merck) was supplied by Merck. Polyethylene terephthalate (PET) was obtained from commercial colorless transparent mineral water bottles. Low-density polyethylene (PE) was provided by DOW and polystyrene (PS) were obtained from packaging tray waste. All of them were cryogenically grinded and sieved to particle smaller than 100 μm.

2.2. Preparation and characterization of support and catalysts

Mono- (Pt) and bimetallic (PtPd and PtRh) catalysts were prepared by sequential wet impregnation using ENS250, ENS350 and Merck as carbon supports. The metal loading was 1.5–3 wt% and the metal molar ratio was 1:1 for the bimetallic catalysts. The impregnated catalysts were dried overnight at 60 °C, calcinated for 2 h at 200 °C, and reduced at 300 °C under H₂ flow. X-ray photoelectron spectroscopy (XPS) profiles of the catalysts were obtained using a PHI Model 5701 Multi-technique System apparatus with an X-ray source, Mg 1253.6 eV std at 300 W, and beam diameter of 720 μm. “XPSpeak v4.1” software was used for peak deconvolution. Data analysis involved smoothing, Shirley background subtraction and mixed Gaussian-Lorentzian by a least-square method for curve fitting. Binding energy correction due to sample charging was carried out using C1s (284.6 eV) peak as an internal standard. The dispersion, morphology and size of the metal nanoparticles were studied by transmission electron microscopy (TEM) with a Tecnai F30 (FEI) microscope. The size of the Pt nanoparticles was measured using J-image software and considering more than 100 nanoparticles from different TEM images. The mean diameter was calculated as $\bar{d} = \left(\sum_i n_i d_i^3 / \sum_i n_i d_i^2 \right)$ and the corresponding error as the standard deviation of the data.

2.3. APR reactions

The APR reactions were performed using batch reactors (BR100, Berghof) at 195–235 °C, 24–32 bar, pH 3–12 under vigorous agitation for 4–8 h. The reaction volume was 15 mL, with a 0.3 g catalyst load, and the plastic load ranged 0.05–0.15 g. The study of the influence of pH was carried out by adjusting the reaction medium pH at 3 and 12, using HCl (1 M) and KOH (1 M) respectively. Before each run, an Ar flow was used to purge air from the reactor and set the initial pressure to 5 bar of gauge pressure. Gas samples were collected in multilayer foil bags (Supelco, USA) and analysed by gas chromatography using FID and TCD detectors (7820A, Agilent Technologies). Previous runs without catalysts and at deionized water pH were performed, and no significant carbon conversion to gas (CC_{gas}) was obtained, indicating a lack of routes in non-catalytic hydrothermal treatment leading to gas products at the temperatures studied.

The CC_{gas} and the H₂ and alkanes yield were calculated as follows:

$$CC_{gas} = \frac{C_{gas}(g)}{C_{initial}(g)} \cdot 100[\%]$$

$$Yield_{(alkanes/H_2)} = \frac{alkanes/H_{2, gas}(mmol)}{PET(g)} [mmol/g]$$

where (C/H₂/alkanes)_{gas} refers to the total moles of C/H₂/alkanes in the gas and C_{initial} corresponds to the theoretical C content in the starting plastic.

Liquid samples were analyzed using a TOC analyzer (Shimadzu TOC-VCSH). Table S1 of the [Supplementary Material](#) shows the TOC of the effluent from selected experiments using PET as feedstock.

3. Results and discussion

3.1. Characterization of fresh catalysts

The structure of the Pt phase in the set of catalysts prepared did not show relevant differences in terms of speciation and size. The formation of an equivalent metallic phase for the fresh catalyst with 1.5 and 3 wt% of Pt is proved by the XPS of the Pt 4f region deconvoluted (Figure S1), showing a similar distribution of Pt species, with Ptⁿ⁺/Pt⁰ ratios of 1.2 and 1.1. The TEM micrographs (Fig. 1a and Figure S2) show characteristic Pt spherical nanoparticles distributed homogeneously over the carbon support for both fresh catalysts. Additionally, the nanoparticles

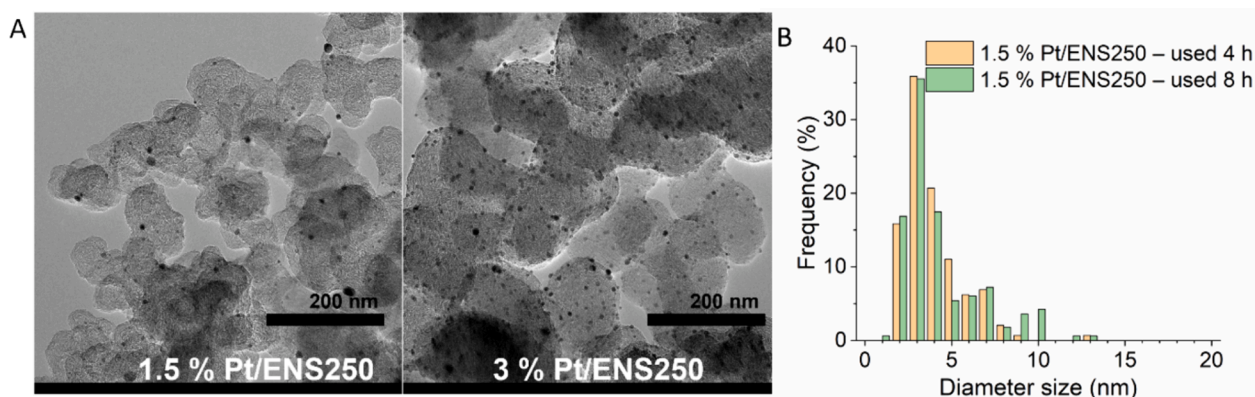


Fig. 1. A) Representative TEM images and B) Pt nanoparticle size distribution of the fresh catalyst 1.5 and 3 % Pt/ENS250.

exhibit similar mean size of 5.4 ± 2.6 and 6.9 ± 3.9 nm for the catalyst with 1.5 and 3 wt% of Pt, respectively, also showing analogous nanoparticle size distribution as depicted by the histograms in Fig. 1b.

3.2. APR experiments

Different plastic materials were screened to identify suitable feedstocks for direct conversion to hydrogen. Fig. 2 shows gas composition, CCgas and yield to valuable gas products in the direct APR of PET, LDPE, and PS with a 1.5 % Pt/ENS250 catalyst. The blank runs show that at 220 °C the plastics undergo limited degradation leading to CCgas (below 0.5 %) and negligible hydrogen in the produced gas. The presence of the catalyst clearly promoted PET and LDPE conversion to gas; however, conversion was significantly lower in the case of PS, as showed by the CCgas and yield to valuable gas products obtained. Direct APR of solid plastic waste has rarely been reported because the APR reaction mechanism is known to occur in the water phase and on the catalyst surface. The melting points of the plastics studied (ca. 250 °C PET, 110 °C LDPE, 240 °C PS) indicate that only LDPE can form a heterogeneous liquid phase in the APR medium, enabling intimate contact with the catalyst. In fact, the catalyst recovered after runs with LDPE was coated by plastic, which is attributable to the interaction of non-polar LDPE liquid droplets and the carbon black used as catalyst support. Despite this interaction, the gas produced from LDPE does not show the usual pattern of APR gas, i.e., higher concentration of hydrogen than alkanes [17]. The results indicate that LDPE undergoes some extent of cracking in the aqueous media, which has also been reported in subcritical water for temperatures above 150 °C even in the absence of a catalyst [18], although in the current work some contribution of catalytic cracking is also expected due to the presence of the Pt catalyst. In any case, the generation of valuable gases by direct APR of LDPE is limited, which is consistent with works in literature exploring pretreatment of polyethylene by oxidation to generate a water-soluble fraction that can be converted to hydrogen by APR [5].

In the case of PS, a very low CCgas value was observed, and the gas produced was mainly composed of CO₂, which can be attributed to hydrothermal carbonization rather than APR, although PS has been reported to undergo only limited carbonization at APR conditions [19]. Likewise, the hydrolysis and depolymerization of PS in aqueous media to light products has been shown to occur significantly only at temperatures well above 300 °C [20], therefore, PS degradation pathways contributing to hydrogen production by direct APR are hampered.

The results for PET suggest that hydrolysis of the plastic in the APR medium can facilitate the route to reforming, although in these screening tests relatively low hydrogen yield was obtained compared to other feedstocks used in APR. It should also be noted that PET is the only plastic studied that contains O in its structure, with a C:O ratio of 2.5. In their pioneering work, Cortright et al. [21] proposed that the production

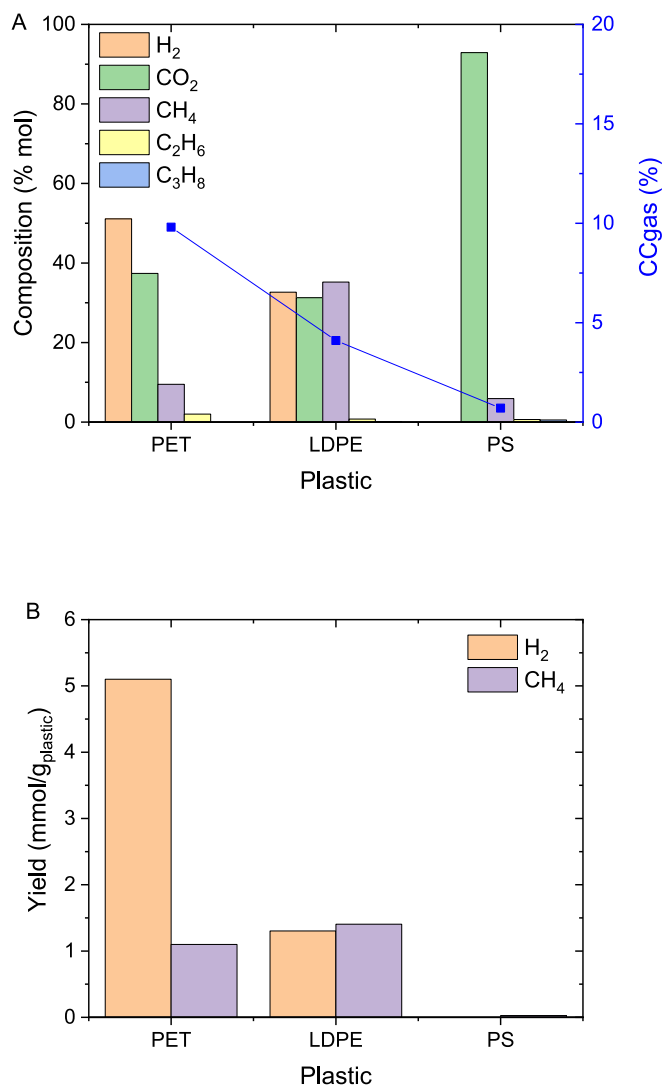


Fig. 2. A) Gas composition and CCgas, and B) yield to gas products, in direct APR of PET, LDPE and PS with 1.5 % Pt/ENS250 catalyst ($W_{\text{PLASTIC}} = 0.1$ g; $W_{\text{CAT}} = 0.3$ g; $T = 220$ °C; $t = 4$ h).

of H₂ from oxygenated hydrocarbons is optimal for compounds with a C:O ratio of 1, with C–C bond cleavage leading to H₂ production and C–O bond cleavage resulting in alkane formation. This feature and the results shown here indicate better processability of PET in APR, which has also been reported by Su et al. [15] using a Ru–ZnO catalyst with metal loads

ranging from 5 to 25 % supported on mesoporous carbon and temperatures between 210 and 250 °C in a two-step process. It was shown that the reaction pathway proceeds through hydrolysis of PET, with ethylene glycol as the main substrate contributing to the production of H₂ by APR.

Further experiments were conducted to assess the sensitivity of direct APR of PET to process variables. Fig. 3 shows gas composition, CCgas and yield to valuable gas products in experiments carried out at different temperatures within the range usually reported for APR of various feedstocks. It can be observed that at 190 °C CCgas has a very low value, slightly above 10 %. Likewise, very low hydrogen yield was obtained, with hydrogen amounting to only about 5 % of the gas produced. The use of a low temperature has been reported for some feedstocks to increase hydrogen selectivity due to lower extent of secondary reactions consuming hydrogen, i.e. side reactions favored at the same T and P conditions of APR, such as the hydrogenation of reaction intermediates [22]. The poor results in the current work at 190 °C suggest that PET is not sufficiently hydrolyzed to intermediates that can be reformed at these mild conditions [23,24]. The gas distribution in the APR shows high production of CO₂ together with alkanes, which could indicate hydrolysis to terephthalic acid followed by degradation to benzoic acid by decarboxylation, and also degradation of ethylenglycol

to acetaldehyde by a dehydration reaction and further decarboxylation [25]. However, the occurrence of these gas products can also be the result of PET hydrothermal carbonization [26]. It is also noteworthy that CO was not detected as a product of any APR reaction, indicating that the water–gas shift reaction is favored in the APR operating conditions.

The increase of APR temperature led to higher CCgas, peaking at 220 °C. Hydrogen production and concentration in the produced gas increased over the whole temperature range considered, particularly from 205 to 220 °C, showing that the APR of the PET hydrolysis products is favored at high temperature and competes with secondary reactions such as hydrothermal carbonization or degradation of PET moieties by decarboxylation and dehydration. Moreover, a slight increase in TOC concentration of the effluent along with temperature was observed (Table S1). The higher contribution of the reforming routes is also evidenced by the decrease in the concentration of carbon dioxide, methane, and ethylene in produced gases. At 235 °C a decrease in CCgas can be observed, suggesting condensation of species and formation of coke-like structures, although the net production of hydrogen increased from 200 to 235 °C due to higher selectivity. Thus, Su et al. [15] reported that the addition to ZnO phase to Ru catalysts prevented deactivation by catalysing the conversion of intermediates adsorbed on the catalyst surface into terephthalic acid and ethylene glycol. Thus, in that study a sustained increase in gas production was observed when temperature was increased up to 250 °C.

The production of gas products in the APR of substrates such as glycerol and maltose has been found to be influenced by the presence of alkalis and acids, although different effects have been reported [27–29]. Therefore, direct APR of PET was studied at different pH values of the starting reaction medium. Fig. 4 shows a minor influence of this variable, with a slight increase in CCgas when the starting pH of the APR reaction medium was increased. Both selectivity and yield to H₂ peaked for a starting pH of 7, with noticeably lower H₂ yield and very high CO₂ concentration for a pH of 12. This pattern, together with the increase in methane production, may indicate a higher contribution of hydrothermal carbonization. At the extreme values of pH the TOC of the effluent (Table S1) was higher than that observed in experiments at pH 7, which could be attributable to a higher level of acid/basic hydrolysis of the PET, but this had minor effect on catalyst behavior, especially at pH 3.

The balance between hydrogen-productive and non-productive reactions may be related to the availability of active centers and reaction intermediates. Therefore, a set of runs was carried out to study the influence of metal load in the catalyst and the plastic-to-catalyst ratio.

The comparison of 1.5 % Pt/ENS250 and 3 % Pt/ENS250 catalysts in Fig. 5 show that a higher metal load led to a higher conversion to gas. This increase is associated with a higher production of CO₂, methane, and ethane, which suggests higher extent of cracking reactions due to the availability of active centers. Likewise, a decrease in hydrogen production can be observed. Su et al. [15] observed a decrease in catalytic performance with increasing active phase content for loads above 10 %, which was attributed to a reduction of surface area. It must be noted that the catalysts used in the current work have very low Pt content, and that for a 1.5 % Pt load, more than 5 mmol/g_{PET} were produced, outperforming Ru-ZnO catalysts with the same metal load.

Fig. 6 shows the CCgas and gas composition obtained in two consecutive cycles of catalyst use. In the second cycle the CCgas diminished by ca. 50 %, H₂ molar concentration decreased by 20 % and CO₂ concentration slightly increased. Also, a marked decrease of 80 % in H₂ yield was observed.

To study the evolution of catalyst behavior with reaction time, 8-hour experiments were carried out. Fig. 7 shows CCgas and gas composition for the 4-hour and 8-hour reaction time experiments. The CCgas increased by 40 % due to the extended reaction time, while the H₂ and CO₂ concentration increased by 15 % and decreased by 12 %, respectively. Interestingly, the H₂ yield increased by 100 % up to 10.1 mol / kg_{PET}. Su et al. reported yields of ca. 20 mmol of H₂/g_{plastic} in the APR of PET but this was achieved at significant higher temperature

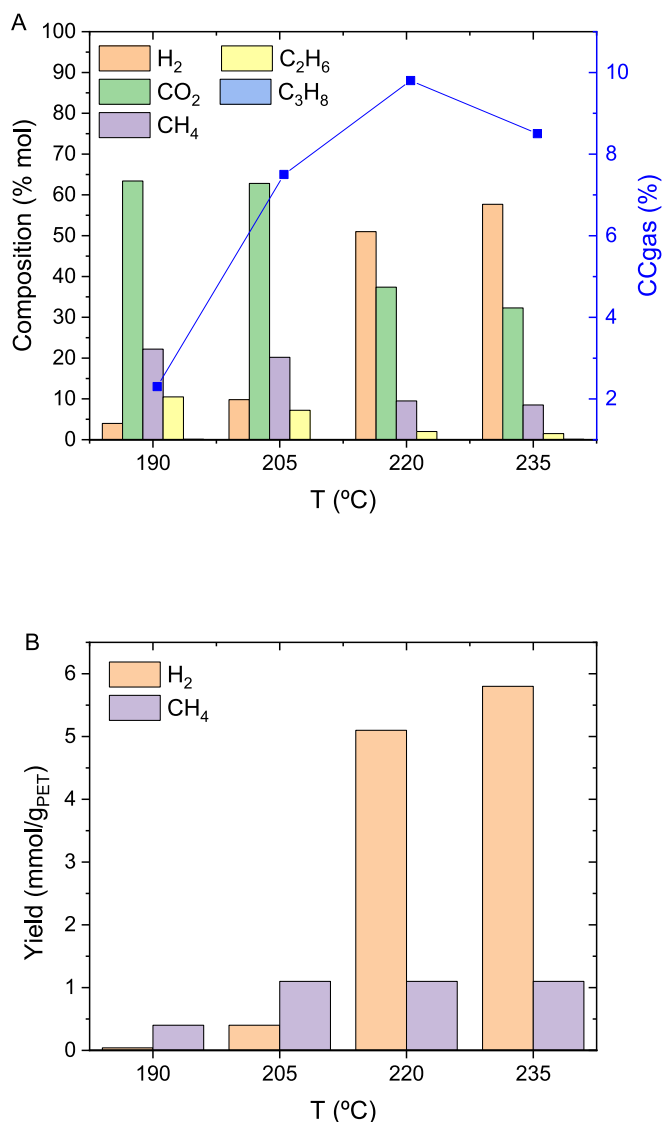


Fig. 3. A) Gas composition and CCgas, and B) yield to gas products, in direct APR of PET at different temperatures (1.5 % Pt/ENS250; W_{PET} = 0.1 g; W_{CAT} = 0.3 g; t = 4 h).

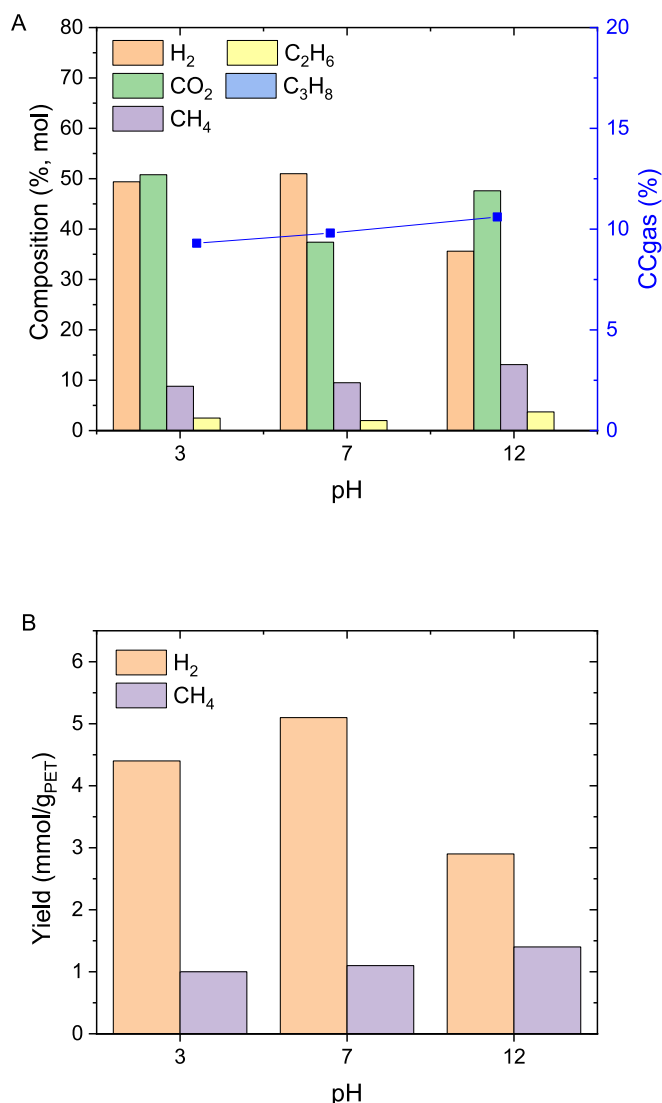


Fig. 4. A) Gas composition and CCgas, and B) yield to gas products, in direct APR of PET at different starting pH (1.5 % Pt/ENS250 catalyst; $W_{\text{PLASTIC}} = 0.1$ g; $W_{\text{CAT}} = 0.3$ g; $T = 220$ °C; $t = 4$ h).

(250 °C) and using a higher metal-loading content of 5 % Ru-ZnO/C catalyst in the consecutive hydrothermal depolymerization and aqueous phase reforming process [15]. Su et al. reported yields of H₂ of 12.2 mmol of H₂ /g_{plastic} using two consecutive steps of hydrothermal depolymerization and APR of mixtures of PVC and PET [30].

These results clearly indicate that the deactivation observed in the catalysts after one use in a 4-hour reaction test could occur during the cooling and drying steps, rather than progressively during the reaction, showing that continuous experiments can be a promising approach.

3.3. Characterization of used catalyst

The catalysts used after 4 and 8 h exhibited some differences compared to the fresh catalyst. The metallic phase showed a slight difference in the distribution of the Pt species, as calculated from the deconvolution of their XPS (Figure S3), with a decrease in the Ptⁿ⁺/Pt⁰ ratio from 1.2 (fresh catalyst) to 1.0 after use for 4 and 8 h. This change can be attributed to a slight Pt reduction during the APR process due to generation of H₂ on the surface of the metal catalyst and the temperature used in the reaction.

Regarding the micrographs obtained by TEM, some nanoparticles

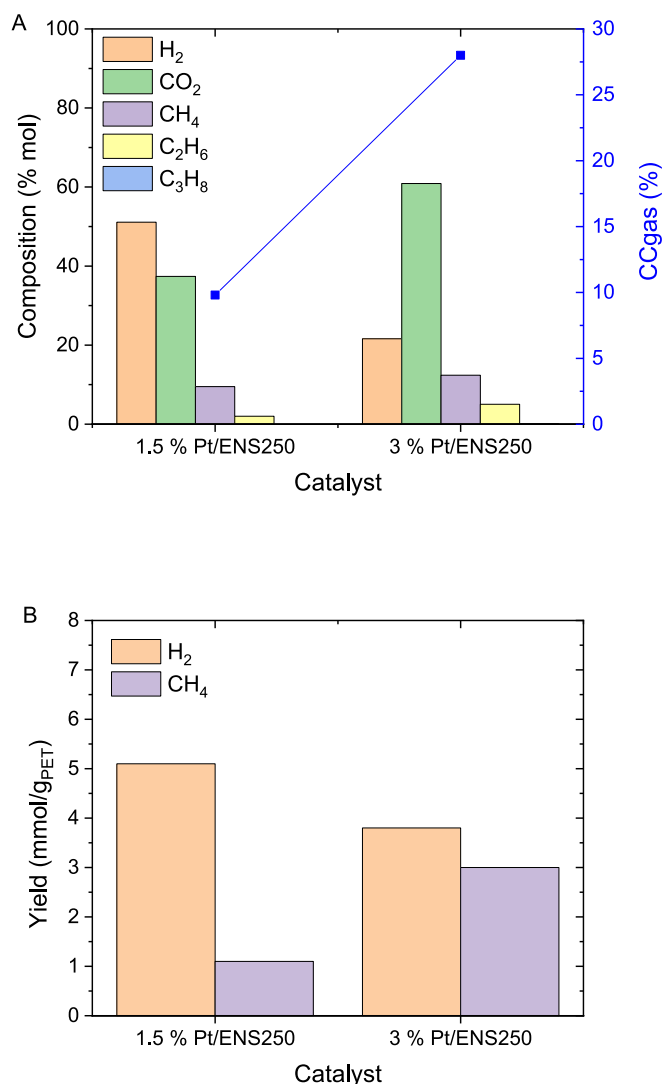


Fig. 5. A) Gas composition and CCgas, and B) yield to gas products, in direct APR of PET with 1.5 % Pt/ENS250 and 3 % Pt/ENS250 catalysts ($W_{\text{PLASTIC}} = 0.1$ g; $W_{\text{CAT}} = 0.3$ g; $T = 220$ °C; $t = 4$ h).

with higher size can be observed in the used catalyst. In general, the distribution of the metallic phase on the carbon support is still homogeneous (Fig. 8); however, the mean nanoparticle size for the 1.5 % Pt/ENS250 catalysts used for 4 and 8 h of reaction shows an increase (10.2 ± 6.0 and 13.8 ± 9.2 nm respectively), indicating a partial agglomeration of the nanoparticles during the process, and also probably some contribution of Ostwald ripening process considering the globular shape of the oversized nanoparticles. Likewise, the mean nanoparticle size is slightly larger for the catalyst used in the 8-hour reaction tests.

Physical mixtures of PET (11 wt%) with ENS250 support and 1.5 % Pt/ENS250 catalyst were studied by TGA to identify the evolution and oxidation pattern for each component. The DGT-TPO curves corresponding to the PET and ENS250 mixture showed two clear peaks at 414 °C and 714 °C, corresponding to the burn-off of PET and ENS250 support, respectively, as shown in Fig. 9b. However, in the profile displayed in the case of the PET-catalyst mixture, the oxidation of the ENS250 carbon was observed at a lower temperature (ca. 450 °C). This difference shows that Pt catalyzes oxidation of the support for Pt/ENS250 catalyst, shifting DGT-TPO support peak to lower temperature, while the PET peak was not affected.

The DGT-TPO profiles of the used 1.5 % Pt/ENS250 catalyst ($T = 220$ °C, neutral starting pH, 0.1 g of PET and 0.3 g of catalysts and 4 h)

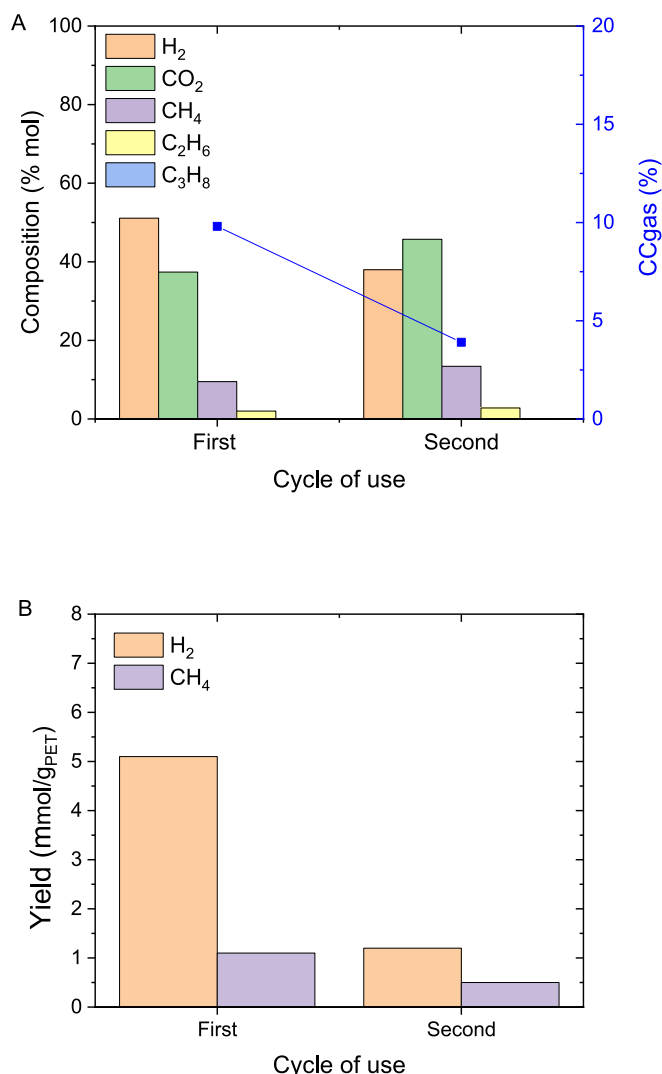


Fig. 6. A) CCgas and gas composition, and B) yield to gas products using PET as substrate with 1.5 % Pt/ENS250 catalyst over cycles of use. ($m_{\text{PET}} = 0.1$ g; $m_{\text{cat}} = 0.3$ g; $T = 220$ °C, $t = 4$ h).

are similar to that of the DGT-TPO of the mixture of PET and fresh 1.5 % Pt/ENS250 catalyst, but a new peak appears corresponding to a weight-loss of ca. 5 % at ca. 275 °C, indicating deposition of organic compounds from PET degradation and non-carbonized condensation matter on the catalyst surface. This matter may be related to deposition during cooling down and drying of the catalyst and can be assumed to be responsible for the dramatic decrease of H₂ production in the second cycle of use. This also suggests that this drawback for the operation in batch mode involving recovery of catalyst for the next step could be avoided in continuous operation mode.

3.4. Catalyst modification for a better APR performance

Once the feasibility of carrying out the direct APR of PET was proved, alternatives regarding the metallic phase and the support were explored to find better-performing catalysts. Thus, two bimetallic catalysts, 1.5 % PtPd/ENS250 and 1.5 % PtRh/ENS250, were explored to assess the effect of the second metal on the catalyst behavior. As shown in Fig. 10a, the use of Pd as the second metal produced a dramatic decrease in CCgas and H₂ concentration in the gas mixture, together with an increase in CO₂ and CH₄ contribution to the gas composition. The high CO₂ fraction in the gas composition suggests that hydrothermal carbonization can be

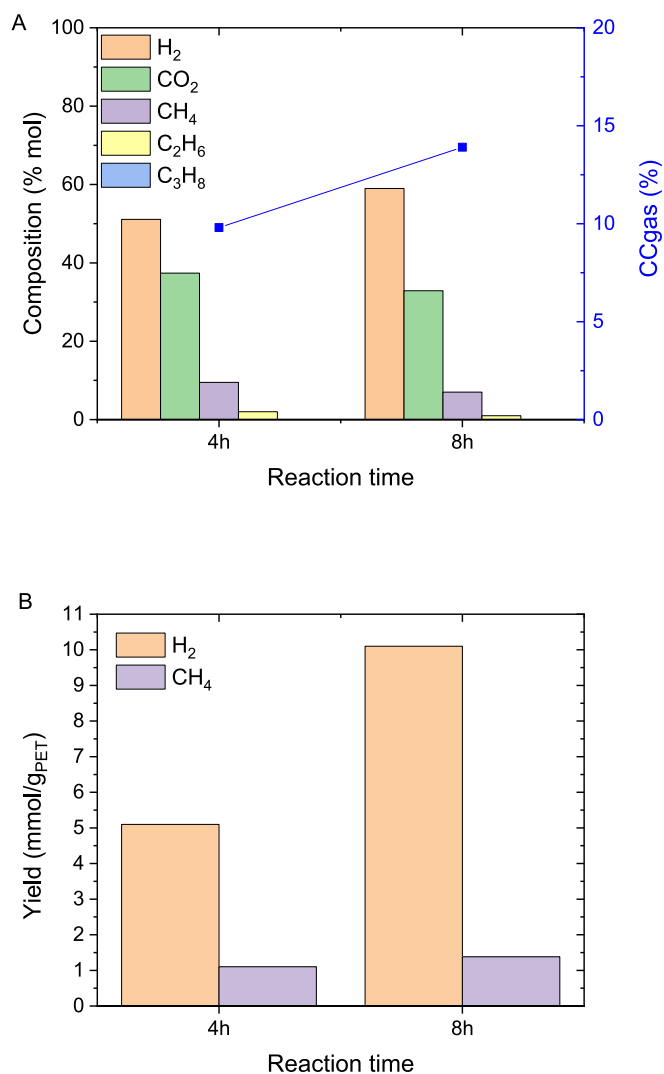


Fig. 7. A) CCgas and gas composition, and B) yield to gas products using PET as substrate using 1.5 % Pt/ENS250 catalyst at different reaction times. ($m_{\text{PET}} = 0.1$ g; $m_{\text{cat}} = 0.3$ g; $T = 220$ °C).

relevant. Likewise, the high methane contribution to the gas composition can be ascribed to methanation, because Pd favors hydrogenation rather than dehydrogenation, compared to other noble metals [31].

In the case of the bimetallic PtRh catalysts, CCgas, and H₂ and CO₂ concentration values were close to those obtained with the monometallic Pt catalyst, but CH₄ concentration was clearly lower, indicating that the bimetallic PtRh catalyst favors H₂ selectivity. This can also be observed in Fig. 10b, where H₂ and CH₄ yields for the three catalysts tested are shown. CH₄ yield for bimetallic PtRh catalysts is 50 % lower than that for monometallic Pt, which can be related to lower activity of PtRh catalyst in methanation routes.

Additional carbon supports were tested to check their effect on catalytic behavior. Fig. 11 shows the gas composition, CCgas and yield to products for Pt catalysts with different supports. The characterization of these supports can be found as Supplementary Material in Table S2. As it can be observed, the use of mesoporous carbon black (ENS350) did increase the H₂ concentration and lowered alkanes production, resulting in higher H₂ selectivity and yield. This could be ascribed to the higher external surface of ENS350 and the corresponding better accessibility of PET hydrolysis and degradation products to metal nanoparticles. The use of activated carbon as support severely affected to the catalyst activity, with much lower values of CCgas and particularly H₂ yield. The results could be attributed to the high microporosity of the activated

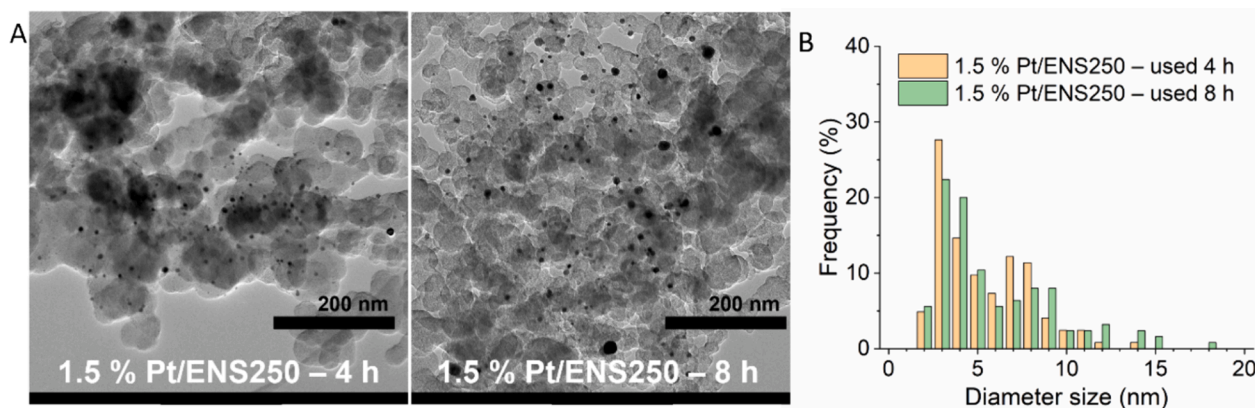


Fig. 8. A) Representative TEM images and B) Pt nanoparticle size distribution of the catalyst 1.5 % Pt/ENS250 used for 4 and 8 h respectively.

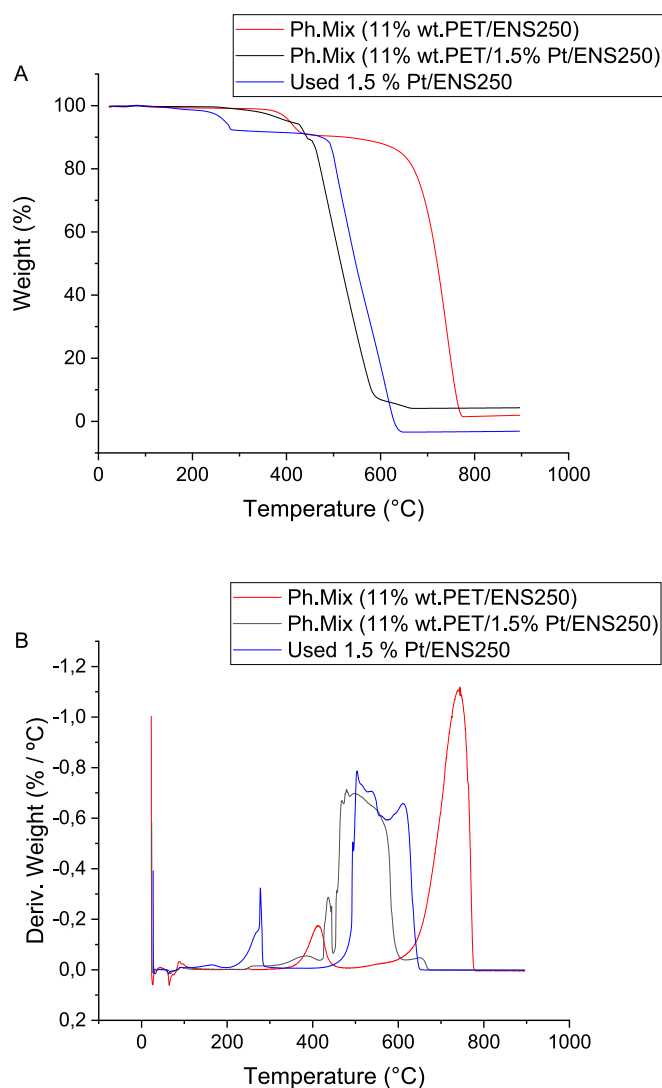


Fig. 9. A) TG-TPO and b) TPO-DTG profiles of a physical mixture of ens250 support and pet (11 wt%), a physical mixture of 1.5 % Pt/ENS250 catalyst and PET (11 wt%) and used 1.5 % Pt/ENS250 catalyst ($T = 220$ °C, neutral pH, 0.1 g of PET, 0.3 g of catalysts, 4 h reaction time).

carbon support, which could hinder the contact between PET hydrolysis and degradation products and the metal phase. CO_2 was the major component in the mixture, whereas methane production was almost

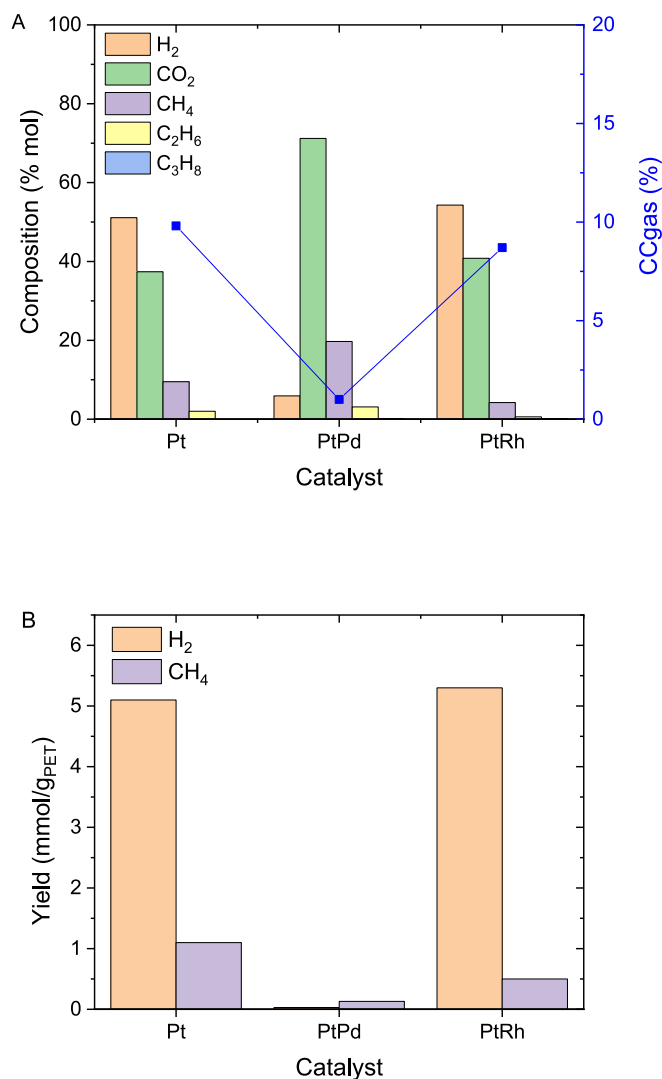


Fig. 10. A) CCgas and gas composition, and B) yield to gas products using PET as substrate using 1.5 % Pt/ENS250, 1.5 % PtPd/ENS250, and 1.5 % PtRh/ENS250 catalysts. ($m_{\text{PET}} = 0.1$ g; $m_{\text{cat}} = 0.3$ g; $T = 220$ °C, $t = 4$ h).

unaffected. Furthermore, the TOC in the effluent is inversely correlated to the mesoporous volume of the catalysts ($\text{ENS350} > \text{Merck} > \text{ENS250}$), evidencing that some of the water-soluble reaction product can be adsorbed onto the support.

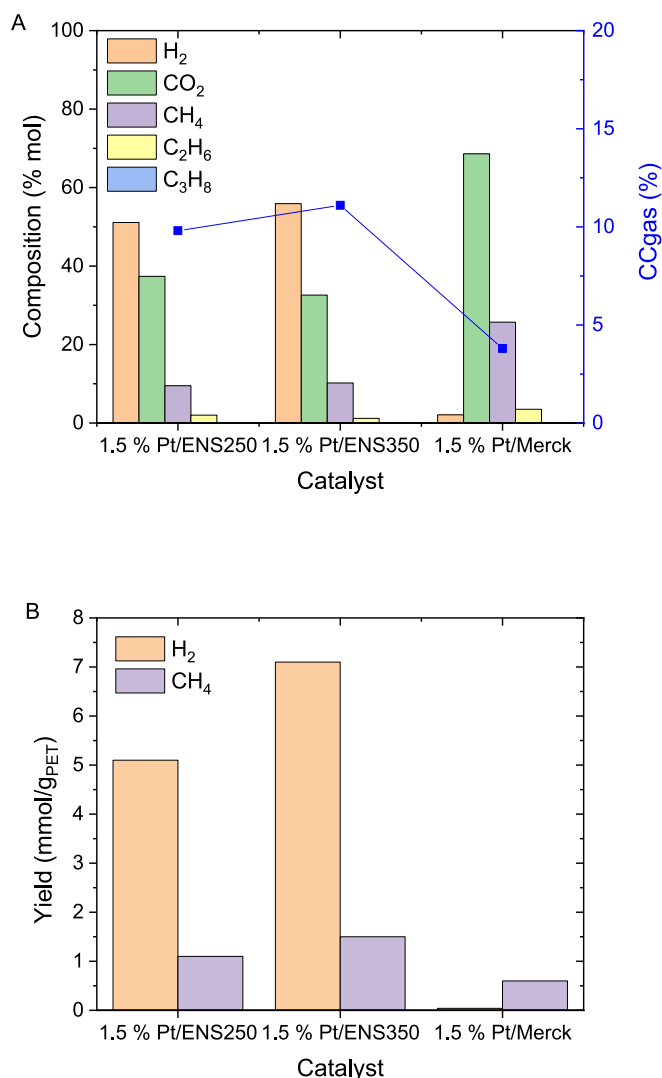


Fig. 11. A) CCgas and gas composition, and B) yield to gas products using PET as substrate using 1.5 % Pt/ENS250, 1.5 % Pt/ENS350, and 1.5 % Pt/Merck catalysts. ($m_{\text{PET}} = 0.1$ g; $m_{\text{cat}} = 0.3$ g; $T = 220$ °C, $t = 4$ h).

The margin for improvement in this research is large despite the relatively high H₂ yields obtained in this exploratory work. Further actions would be directed towards gaining an in-depth understanding of catalysts behavior in long reaction runs, using complex mixtures of plastic as substrates, and more affordable metals as catalysts.

4. Conclusions

The aqueous-phase reforming of three common plastics, polyethylene terephthalate (PET), polystyrene (PS) or polyethylene (PE), was studied, being PET the most favorable to be reformed, whereas mainly hydrothermal carbonization occurred with PS and competing cracking and aqueous-phase reforming were observed in the case of LDPE. A systematic study of the operating conditions, using PET as feedstock, revealed that H₂ production was higher at 235 °C, showing that the aqueous-phase reforming of the PET hydrolysis products is favored at high temperature and competes with secondary reactions. The pH of the starting reaction medium showed minor influence, although a pH of 7 increased H₂ production. The increase of Pt content in the catalyst, from 1.5 to 3 wt%, led to an increase in cracking reactions that slightly lowered H₂ yield. The reuse of the 4-hour-used catalyst led to a 80 % drop in H₂ yield, from 5 to 1 mmol H₂/g_{PET}, whereas an 8-hour

reaction for the same catalyst led to a H₂ yield of 10 mmol H₂/g_{PET}. These results indicate that in batch mode, catalyst deactivation most likely occurs during cooling down and drying steps, making continuous systems a promising approach. The use of PtRh bimetallic catalysts and supports with higher specific surface area and mesoporosity (ENS350) showed great improvement in terms of H₂ yield, suggesting further improvements can be made through catalyst tailoring.

CRediT authorship contribution statement

C. Ruiz-García: Writing – original draft, Investigation, Formal analysis. **J.A. Baeza:** Investigation, Formal analysis, Writing – review & editing. **A.S. Oliveira:** Investigation, Formal analysis. **S. Roldán:** Writing – original draft, Investigation. **L. Calvo:** Validation, Funding acquisition, Conceptualization. **M.A. Gilarranz:** Supervision, Funding acquisition.

Declaration of competing interest

The authors declare that they have no known competing financial interests or personal relationships that could have appeared to influence the work reported in this paper.

Data availability

Data will be made available on request.

Acknowledgements

Authors greatly appreciate funding from Madrid Regional Government (Project S2018/EMT-4344). C. Ruiz-García acknowledges funding from the European Union's Horizon 2020 research and innovation programme under the Marie Skłodowska-Curie grant agreement GA 101064359. A.S. Oliveira thanks the Ministry of Universities; The Recovery, Transformation and Resilience Plan, and the Autonomous University of Madrid for a research grant (CA1/RSUE/2021-00836).

Appendix A. Supplementary data

Supplementary data to this article can be found online at <https://doi.org/10.1016/j.fuel.2024.132446>.

References

- [1] Horton AA. Plastic pollution: when do we know enough? *J Hazard Mater* 2022;422:126885. <https://doi.org/10.1016/j.jhazmat.2021.126885>.
- [2] Ye S, Cheng M, Zeng G, Tan X, Wu H, Liang J, et al. Insights into catalytic removal and separation of attached metals from natural-aged microplastics by magnetic biochar activating oxidation process. *Water Res* 2020;179:115876. <https://doi.org/10.1016/j.watres.2020.115876>.
- [3] Prata JC, Silva ALP, da Costa JP, Mouneyrac C, Walker TR, Duarte AC, et al. Solutions and integrated strategies for the control and mitigation of plastic and microplastic pollution. *Int J Environ Res Public Health* 2019;16:2411. <https://doi.org/10.3390/ijerph16132411>.
- [4] da Costa JP, Santos PSM, Duarte AC, Rocha-Santos T. (Nano)plastics in the environment – sources, fates and effects. *Sci Total Environ* 2016;566–567:15–26. <https://doi.org/10.1016/j.scitotenv.2016.05.041>.
- [5] Su H, Li T, Zhu L, Wang S. Catalytic reforming of the aqueous phase derived from diluted hydrogen peroxide oxidation of waste polyethylene for hydrogen production. *ChemSusChem* 2021;14:4270–9. <https://doi.org/10.1002/cssc.202100913>.
- [6] <https://plasticseurope.org/knowledge-hub/plastics-the-facts-2022/> (accessed 13/04/2023).
- [7] Haider TP, Völker C, Kramm J, Landfester K, Wurm FR. Plastics of the future? The impact of biodegradable polymers on the environment and on society. *Angew Chem Int Ed* 2019;58:50–62. <https://doi.org/10.1002/anie.201805766>.
- [8] King S, Locock KES. A circular economy framework for plastics: a semi-systematic review. *J Clean Prod* 2022;364:132503. <https://doi.org/10.1016/j.jclepro.2022.132503>.
- [9] Xu D, Yang S, Su Y, Xiong Y, Zhang S. Catalytic conversion of plastic wastes using cost-effective bauxite residue as catalyst into H₂-rich syngas and magnetic

- nanocomposites for chrome(VI) detoxification. *J Hazard Mater* 2021;413:125289. <https://doi.org/10.1016/j.jhazmat.2021.125289>.
- [10] Qureshi MS, Oasmaa A, Pihkola H, Deviatkin I, Tenhunen A, Mannila J, et al. Pyrolysis of plastic waste: opportunities and challenges. *J Anal Appl Pyrolysis* 2020;152:104804. <https://doi.org/10.1016/j.jaap.2020.104804>.
 - [11] Lopez G, Artetxe M, Amutio M, Alvarez J, Bilbao J, Olazar M. Recent advances in the gasification of waste plastics. A critical overview. *Renew Sustain Energy Rev* 2018;82:576–96. <https://doi.org/10.1016/j.rser.2017.09.032>.
 - [12] Parku GK, Collard F, Görgens JF. Pyrolysis of waste polypropylene plastics for energy recovery: influence of heating rate and vacuum conditions on composition of fuel product. *Fuel Process Technol* 2020;209:106522. <https://doi.org/10.1016/j.fuproc.2020.106522>.
 - [13] Plastics to Fuel Developer's Guide. Ocean Recovery Alliance. 2015. https://www.oceanrecov.org/assets/files/Valuing_Plastic/2015-PTF-Project-Developers-Guide.pdf (accessed 13/04/2023).
 - [14] Pipitone G, Zoppi G, Pirone R, Bensaid S. A critical review on catalyst design for aqueous phase reforming. *Int J Hydrogen Energy* 2022;47:151–80. <https://doi.org/10.1016/j.ijhydene.2021.09.206>.
 - [15] Su H, Hu Y, Feng H, Zhu L, Wang S. Efficient H₂ production from PET plastic wastes over mesoporous carbon-supported Ru-ZnO catalysts in a mild pure-water system. *ACS Sustainable Chem Eng* 2023;11:578–86. <https://doi.org/10.1021/acssuschemeng.2c05062>.
 - [16] Oliveira AS, Sarrión A, Baeza JA, Diaz E, Calvo L, Mohedano AF, et al. Integration of hydrothermal carbonization and aqueous phase reforming for energy recovery from sewage sludge. *Chem Eng J* 2022;442:136301. <https://doi.org/10.1016/j.cej.2022.136301>.
 - [17] Coronado I, Stekrova M, Reinikainen M, Simell P, Lefferts L, Lehtonen J. A review of catalytic aqueous-phase reforming of oxygenated hydrocarbons derived from biorefinery water fractions. *Int J Hydrogen Energy* 2016;41:11003–32. <https://doi.org/10.1016/j.ijhydene.2016.05.032>.
 - [18] Wong SL, Ngadi N, Amin NAS, Abdullah TAT, Inuwa IM. Pyrolysis of low density polyethylene waste in subcritical water optimized by response surface methodology. *Environ Technol* 2016;37:245–54. <https://doi.org/10.1080/09593330.2015.1068376>.
 - [19] Zhao X, Zhan L, Xie B, Gao B. Products derived from waste plastics (PC, HIPS, ABS, PP and PA6) via hydrothermal treatment: characterization and potential applications. *Chemosphere* 2018;207:742–52. <https://doi.org/10.1016/j.chemosphere.2018.05.156>.
 - [20] Bai B, Jin H, Fan C, Cao C, Wei W, Cao W. Experimental investigation on liquefaction of plastic waste to oil in supercritical water. *Waste Manage* 2019;89:247–53. <https://doi.org/10.1016/j.wasman.2019.04.017>.
 - [21] Cortright RD, Davda RR, Dumesic JA. Hydrogen from catalytic reforming of biomass-derived hydrocarbons in liquid water. *Nature* 2002;418:964–7. <https://doi.org/10.1038/nature01009>.
 - [22] Oliveira AS, Aho A, Baeza JA, Calvo L, Simakova IL, Gilarranz MA, et al. Enhanced H₂ production in the aqueous-phase reforming of maltose by feedstock pre-hydrogenation. *App Catal B: Environ* 2021;281:119469. <https://doi.org/10.1016/j.apcatb.2020.119469>.
 - [23] Tuna Ö, Bal A, Güçlü G. Investigation of the effect of hydrolysis products of postconsumer polyethylene terephthalate bottles on the properties of alkyd resins. *Polym Eng Sci* 2013;53:176–82. <https://doi.org/10.1002/pen.23247>.
 - [24] Muhammad SI, Islam Z, Hasan R, Shofiul Islam MJAHM. Acidic hydrolysis of recycled polyethylene terephthalate plastic for the production of its monomer terephthalic acid. *Prog Rub, Plast Recycl Technol* 2023;39:12–25. <https://doi.org/10.1177/14777606221128038>.
 - [25] Čolnik M, Pečar D, Knez Ž, Goršek A, Škerget M. Kinetics study of hydrothermal degradation of PET waste into useful products. *Processes* 2022;10. <https://doi.org/10.3390/pr10010024>.
 - [26] Xu Z, Bai X. Microplastic degradation in sewage sludge by hydrothermal carbonization: efficiency and mechanisms. *Chemosphere* 2022;297:134203. <https://doi.org/10.1016/j.chemosphere.2022.134203>.
 - [27] Remón J, Ruiz J, Oliva M, García L, Arauzo J. Effect of biodiesel-derived impurities (acetic acid, methanol and potassium hydroxide) on the aqueous phase reforming of glycerol. *Chem Eng J* 2016;299:431–48. <https://doi.org/10.1016/j.cej.2016.05.018>.
 - [28] Remón J, Jarauta-Córdoba C, García L, Arauzo J. Effect of acid (CH₃COOH, H₂SO₄ and H₃PO₄) and basic (KOH and NaOH) impurities on glycerol valorisation by aqueous phase reforming. *App Catal B: Environ* 2017;219:362–71. <https://doi.org/10.1016/j.apcatb.2017.07.068>.
 - [29] Oliveira AS, Baeza JA, García D, Saenz de Miera B, Calvo L, Rodríguez JJ, et al. Effect of basicity in the aqueous phase reforming of brewery wastewater for H₂ production. *Renew Energy* 2020;148:889–96. <https://doi.org/10.1016/j.renene.2019.10.173>.
 - [30] Su H, Wu Y, Pan J, Zhu L, Wang S, Hu Y. High-purity H₂ production from mixed PVC/PET plastic wastes through tandem hydrothermal depolymerization and aqueous phase reforming. *Process Saf Environ Prot* 2024;184:1282–92. <https://doi.org/10.1016/j.psep.2024.02.068>.
 - [31] Dobrezberger K, Bosters J, Moser N, Yigit N, Nagl A, Föttinger K, et al. Hydrogenation on palladium nanoparticles supported by graphene nanoplatelets. *J Phys Chem C* 2020;124:23674–82. <https://doi.org/10.1021/acs.jpcc.0c06636>.